Tomasz RYMARCZYK[1,2], Barbara STEFANIAK[1], Konrad KANIA[1,2], Michał MAJ[1,2], Konrad NIDERLA[1,2]

Research & Development Centre Netrix S.A.(1), University of Economics and Innovation (2)

doi:10.15199/48.2020.07.23

Implementing deterministic methods to solve the inverse problem for the model with lungs and heart in the EIT

***Abstract**. The article presents the implementation of deterministic methods to solve the inverse problem for a human chest model with lungs and heart in electrical impedance tomography (EIT). It is a non-invasive imaging method involving the examination of an unknown physical object using electric currents and appropriate measurements of voltage drops at its edge. The solution is part of an advanced biomedical application system. The gathering of tomographic data must be fairly fast and reliable so that the algorithms can reconstruct the images in real time. The presented algorithms allow lung and heart monitoring.*

***Streszczenie.** W artykule przedstawiono wdrożenie deterministycznych metod do rozwiązania zagadnienia odwrotnego dla modelu klatki piersiowej człowieka z płucami i sercem w tomografii impedancji elektrycznej. Jest to nieinwazyjna metoda obrazowania polegająca na badaniu nieznanego obiektu fizycznego za pomocą prądów elektrycznych i odpowiednich pomiarów spadków napięcia na jego brzegu. Rozwiązanie jest częścią zaawansowanego systemu aplikacji biomedycznej. Gromadzenie danych tomograficznych musi być dosyć szybkie i niezawodne, aby algorytmy mogły rekonstruować obrazy w czasie rzeczywistym. Przedstawione algorytmy umożliwiają monitorowanie płuc i serca. (**Implementacja metod deterministycznych do rozwiązania zagadnienia odwrotnego dla modelu z płucami i sercem w ETI)**.*

Keywords: electrical tomography; image reconstruction; biomedical signal.
Słowa kluczowe: tomografia elektryczna; rekonstrukcja obrazu; sygnał biomedyczny.

Numerical model

There are many methods for solving optimization problems [1-13]. The article presents and implements deterministic methods [14-19]. Monitoring lungs in unconscious intensive care patients, collecting data across the entire body border is impractical. The boundary area available for electrical tomography measurements is limited. Physiological processes that cause changes in the electrical conductivity of the body can be monitored using algorithms [20-24]. The proposed approach is to solve the problem of non-linear reconstruction of the inverse image [25-31].

Regularization methods

Methods based on the SVD distribution

(1) $\min_x \left\{ \left\| Ax - b \right\|_2^2 + \lambda^2 \|L(x - x^*)\|_2^2 \right\}$

In the case of EIT, it can consider the sensitivity matrix as A, x the searched permittivity distribution, a b as a measurement vector. In regularization methods, the SVD or GSVD distribution can be used.

We are considering the decomposition SVD ($A = U\Sigma V^T$) for $L = I$, and decomposition GSVD

(2) $A = U \begin{pmatrix} \Sigma & 0 \\ 0 & I \end{pmatrix} X^{-1}, L = V(M, 0)X^{-1}$ for $L \neq I$.

The case considered $L = I$.

Methods based on the SVD distribution

- Tikhonov regularization

For $x^* = 0$ a character solution is got

(3) $x = \sum_{i=1}^{n} \frac{\sigma_i}{\sigma_i^2 + \lambda^2} u_i^T b v_i$(3)

For $x^* \neq 0$

(4) $x = \sum_{i=1}^{n} \frac{\sigma_i}{\sigma_i^2 + \lambda^2} u_i^T b v_i + \frac{\lambda_i^2}{\sigma_i^2 + \lambda^2} x^*$

- DSVD method

For $x^* = 0$ a solution is got

(5) $x = \sum_{i=1}^{n} \frac{u_i^T b}{\sigma_i + \lambda_i} v_i$

For $x^* \neq 0$

(6) $x = \sum_{i=1}^{n} \frac{u_i^T b}{\sigma_i + \lambda_i} v_i + \frac{\lambda_i}{\sigma_i + \lambda_i} x^*$

- TSVD method

We use matrix submatrices U $- U_\lambda = U(:, 1:\lambda)$ and for the matrix V $- V_\lambda = V(:, 1:\lambda)$.

For $x^* = 0$ a solution is got

(7) $x = \sum_{i=1}^{\lambda} \frac{u_{\lambda i}^T b}{\sigma_i} v_{\lambda i}$

Reconstructions

For the presented methods, the values shown in Fig. 1 for heart and lungs as a linear combination of the inverse of the absolute value and the logarithm of the value.. Figure 1 shows the reconstruction of the image by Tikhonov method. Algorithms based on SVD distribution of the sensitivity matrix lead to similar reconstructions. However, the TSVD method leads to the worst reconstruction. Promising reconstructions were obtained by maximum entropy and conjugate gradient methods, the lungs and heart are clearly visible, but the difference between the permeability of these organs is also visible.

For the given model, the parameters for each of its parts have been adopted:

- heart - 0.3332,
- lungs - 0.2844,
- skin - 0.1,
- the zone between organs and the skin - 1.

Several reconstruction methods have been considered. For everyone it appeared that the heart is connected to the lungs. There was no such situation for a model without a skin layer. For the methods discussed, the following reconstructions as shown in Fig. 2-5 were obtained. For the TSVD method with the determined cut-off threshold, the L or quasi curve method optimally does not obtain acceptable reconstructions. The TSVD method with a threshold determined as fitting two straight lines, a parabola for standard deviations of the solution vectors, we obtain a reconstruction (Fig. 5). The methods described above resulted in similar reconstructions.

A function generating an environment with a "diameter" of k for triangular elements was calculated. Examples of designated neighbourhoods for selected elements for "diameters" k = 1,2 (Fig. 6).

Based on neighbourhoods, one can define base vectors ([0,1], [1,1], [1,0], [1, -1]) as a rope combination of selected vectors from the set of generated vectors (the method of generating them is presented in Fig 7).

a)

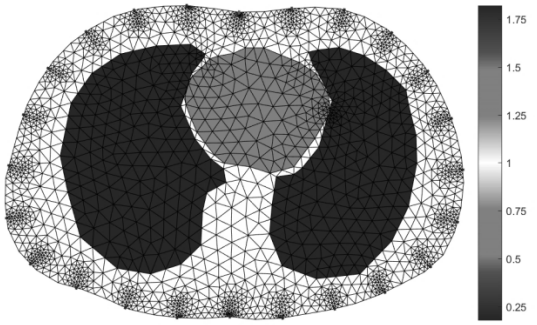

b)

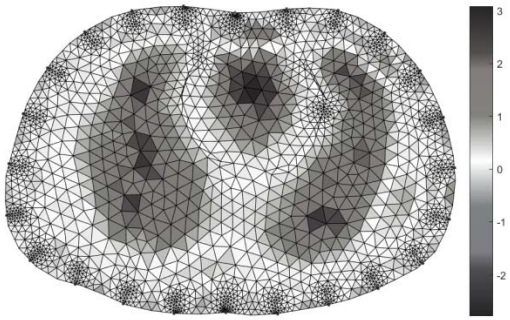

c)

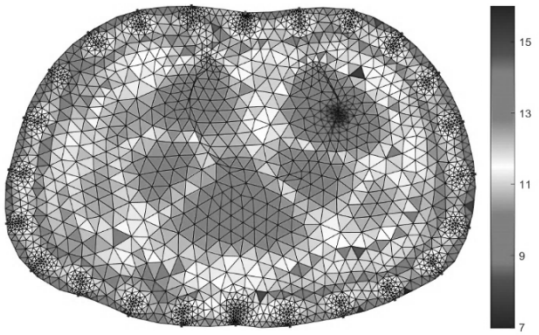

d)

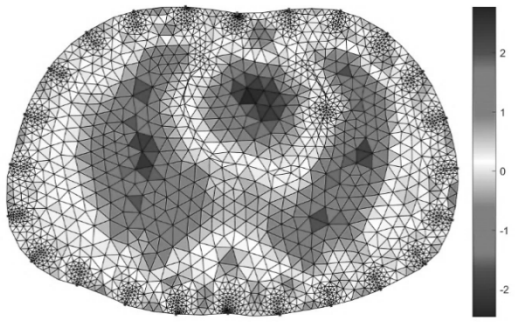

e)

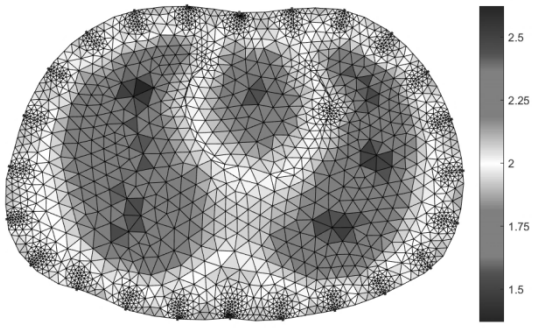

f)

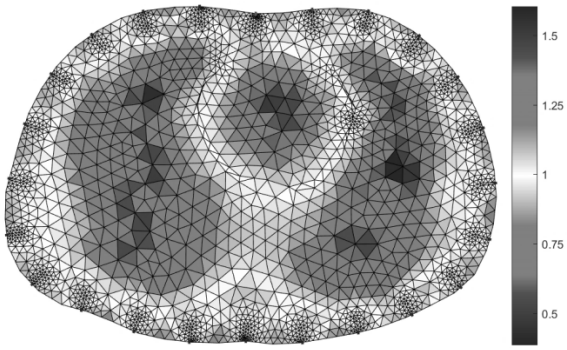

Fig. 1. Image reconstruction: a) 2D model of the lungs and heart, b) Tikhonov method, c) TSVD method, d) DSVD method, e) maximum entropy method, f) conjugate gradient method.

Models with lungs, heart and intervals in armpits (Fig. 2).

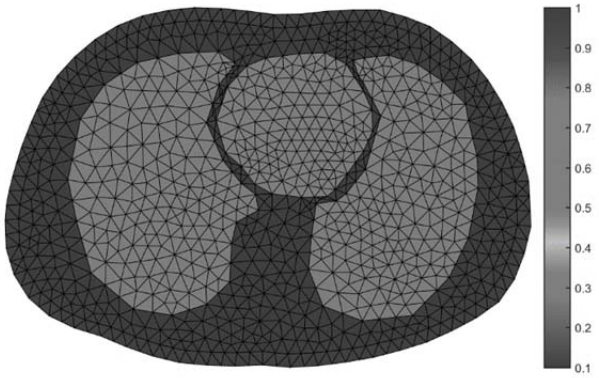

Fig. 2. Model with lungs, heart and intervals on the armpits.

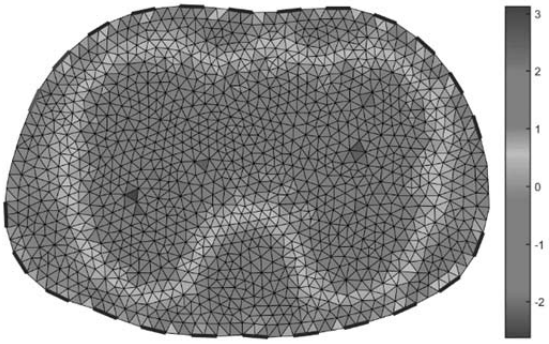

Fig.3. Image reconstruction - the Tikhonov method.

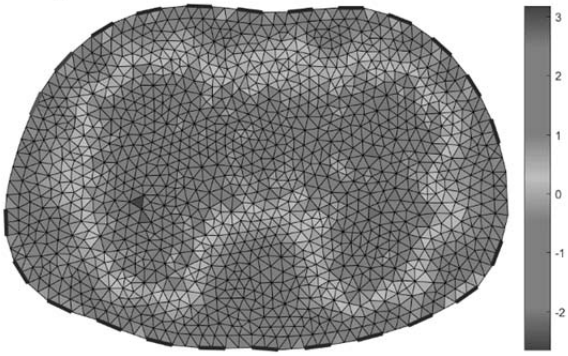

Fig. 4. Image reconstruction - DSVD method.

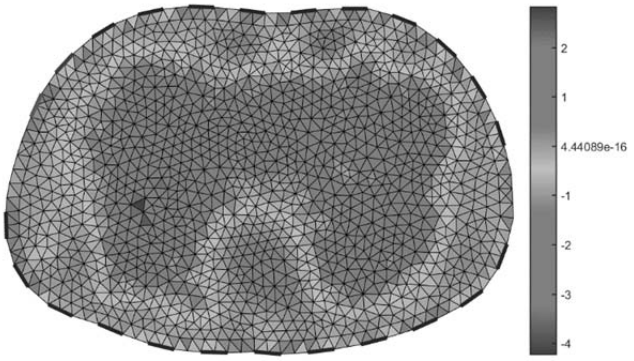

Fig. 5. Image reconstruction - TSVD method.

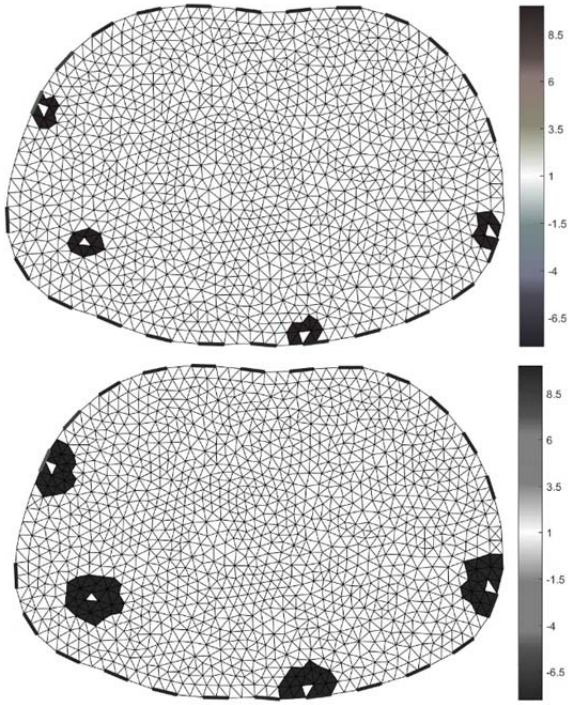

Fig. 6. Examples of designated neighbourhoods for selected elements for diameters k = 1,2.

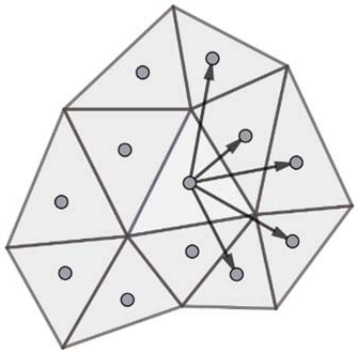

Fig. 7. Basic vectors.

V Vectors are generated as vectors with their origin in the centre of the circle entered for the central element and the end in the centre of the circle entered for each neighbouring element. These operations generate the L matrix ($N \times N$, *N*- number of elements in the grid) filtering the filter (F 3×3) where the elements of this matrix are responsible for the values of the coefficients of linear combinations of vectors generated representing base vectors.

(8) $l_{i,j} = \begin{cases} \sum_{v \in B} a_{i,j}^{v} \cdot F([4,7,8,9,6,3,2,1]) \\ 0, when\ element\ i\ is\ not\ adjacent\ to\ j \end{cases}$,

where: $\boldsymbol{B}$ – set of base vectors
$\boldsymbol{B} =$
$\{[0,1],[1,1],[1,0],[1,-1],[0,-1],[-1,-1],[-1,0],[-1,1]\}$.
$a_{i,j}^{v} = g_j \cdot b_j^{v}$, $v = \sum_{g_k \in S_i} b_k^{v} \cdot g_k$, $\boldsymbol{g}_k -$ one of the vectors generated, $\boldsymbol{S}_i$ – is a set of all vectors generated for an element i (central element Fig. 7).
For character filters $\mathbf{F} = \begin{bmatrix} -a & a & -a \\ a & a & a \\ -a & a & -a \end{bmatrix}$ and for $a = 15$, the reconstruction R was obtained

(9) $\mathbf{R} = (2\mathbf{S}^T\mathbf{S} + \alpha^2 \cdot \mathbf{L}^T\mathbf{L})^{-1} \cdot (2\mathbf{S}^T\boldsymbol{b})$,
where: $\mathbf{S}$ – sensitivity matrix, $\alpha = 2e-4$, $\boldsymbol{b}$ – measurements.

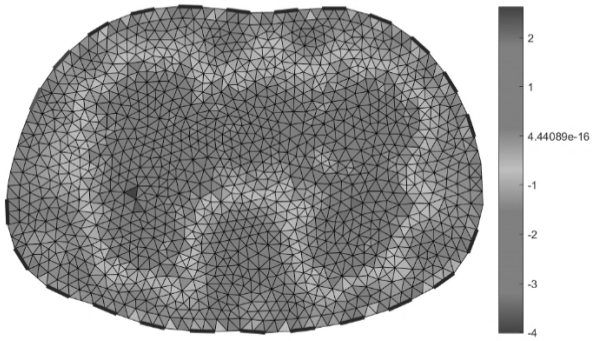

Fig. 8. Reconstruction with the L matrix is a method with GSVD distribution for the S and L matrices.

Reconstruction with the L matrix is a method with the GSVD distribution for the S and L matrices (Fig. 8). Recursive methods such as CAV (Component-averaging), Cimmino, drop (Diagonally Relaxed Orthogonal Projections) and Landwerberg lead to similar reconstructions as the Tikhonov, TSVD and DSVD methods, due to this fact their results have not been presented.

Conclusion

The article presents algorithms for image reconstruction for a human chest model with lungs and heart. Electrical impedance tomography was used for this purpose. It is a non-invasive imaging method involving the examination of an unknown object using electric currents and appropriate measurements of voltage drops at its edge. In medical clinical trials and practice, imaging has become an important part of diagnosing and studying the anatomy and function of the human body. The proposed methods were used to obtain real reconstructions. Data acquisition must be as fast as reliable. The solution is part of an advanced biomedical application system.

***Authors**: Tomasz Rymarczyk, Ph.D. Eng., University of Economics and Innovation, Projektowa 4, Lublin, Poland/ Research & Development Centre Netrix S.A. E-mail: tomasz@rymarczyk.com; Barbara Stefaniak, Research & Development Centre Netrix S.A., E-mail: barbara.stefaniak@netrix.com.pl; Konrad Kania, University of Economics and Innovation, Projektowa 4, Lublin, Poland/ Research & Development Centre Netrix S.A. E-mail: konrad.kania@netrix.com.pl; Michał Maj, University of Economics and Innovation, Projektowa 4, Lublin, Poland/ Research & Development Centre Netrix S.A. E-mail: michal.maj@wsei.lublin.pl; Konrad Niderla, University of Economics and Innovation, Projektowa 4, Lublin, Poland/ Research & Development Centre Netrix S.A. E-mail: konrad.niderla@netrix.com.pl*

REFERENCES

[1] Rymarczyk T., Stefaniak B., Kania K., Maj M., Nita P., Inverse problem solution for model with lungs and heart in EIT, 2019 Applications of Electromagnetics in Modern Engineering and Medicine, PTZE 2019, 2019, 2019, 180-183

[2] Babout L., Grudzień K., Wiącek J., Niedostatkiewicz M., Karpiński B., Szkodo M., Selection of material for X-ray tomography analysis and DEM simulations: comparison between granular materials of biological and non-biological origins, Granular Matter, 20 (2018), No. 3, 20:38.

[3] Banasiak R., Wajman R., Jaworski T., Fiderek P., Fidos H.,; Nowakowski J., Study on two-phase flow regime visualization and identification using 3D electrical capacitance tomography and fuzzy-logic classification, International Journal of Multiphase Flow, 58 (2014), 1-14.

[4] Fiala P., Drexler P., Nešpor D., Szabó Z., Mikulka J., Polívka J., The Evaluation of Noise Spectroscopy Tests, ENTROPY, 18 (2016), No. 12, 1-16.

[5] Krawczyk A., Korzeniewska E., Łada-Tondyra E., Magnetophosphenes – History and contemporary implications, Przeglad Elektrotechniczny, 94 (2018), No 1, 61-64.

[6] Korzeniewska E., Szczesny A., Krawczyk A., Murawski P., Mroz J., Seme S., Temperature distribution around thin electroconductive layers created on composite textile substrates, Open Physics, 16 (2018), No. 1, 37-41.

[7] Rymarczyk, T.; Kozłowski, E.; Kłosowski, G.; Niderla, K. Logistic Regression for Machine Learning in Process Tomography, Sensors, 19 (2019), 3400.

[8] Rymarczyk T., Adamkiewicz P., Polakowski K., Sikora J., Effective ultrasound and radio tomography imaging algorithm for two-dimensional problems, Przegląd Elektrotechniczny, 94 (2018), No 6, 62-69

[9] Kozłowski E., Mazurkiewicz D., Żabiński T., Prucnal S., Sęp J., Assessment model of cutting tool condition for real-time supervision system, Eksploatacja i Niezawodnosc – Maintenance and Reliability, 21 (2019); No 4, 679–685

[10] Li X, Li J, He D, Qu Y. Gear pitting fault diagnosis using raw acoustic emission signal based on deep learning. Eksploatacja i Niezawodnosc – Maintenance and Reliability, 21 (2019), No. 3, 403–410

[11] Szczęsny A.; Korzeniewska E., Selection of the method for the earthing resistance measurement, Przegląd Elektrotechniczny, 94 (2018),No. 12, 178-181.

[12] Vališ, D., Mazurkiewicz, D., Application of selected Levy processes for degradation modelling of long range mine belt using real-time data. Archives of Civil and Mechanical Engineering, 18 (2018), No. 4, 1430-1440.

[13] Valis D., Mazurkiewicz D., Forbelska M., Modelling of a Transport Belt Degradation Using State Space Model, Conference: IEEE International Conference on Industrial Engineering and Engineering Management (IEEE IEEM)Location: Singapore, Dec. 10-13, 2017, Book Series: International Conference on Industrial Engineering and Engineering Management IEEM, 2017, 949-953.

[14] Calderón A. P., On an inverse boundary value problem, Computational & Applied Mathematics, 25 (2006), 133 – 138.

[15] Kryszyn J., Smolik W., Toolbox for 3d modelling and image reconstruction in electrical capacitance tomography, Informatyka, Automatyka, Pomiary w Gospodarce i Ochronie Środowiska (IAPGOŚ), 7 (2017), No. 1, 137-145.

[16] Vališ D, Hasilová K., Forbelská M, Vintr Z, Reliability modelling and analysis of water distribution network based on backpropagation recursive processes with real field data, Measurement 149 (2020), 107026

[17] Mosorov V., Grudzień K., Sankowski D., Flow velocity measurement methods using electrical capacitance tomography, Informatyka, Automatyka, Pomiary w Gospodarce i Ochronie Środowiska (IAPGOŚ), 7 (2017), No.1 ,30-36

[18] Kowalska A., Banasiak R., Romanowski A., Sankowski D., Article 3D-Printed Multilayer Sensor Structure for Electrical Capacitance Tomography, 19 (2019), Sensors, 3416

[19] Chen B., Abascal J., Soleimani M., Electrical Resistance Tomography for Visualization of Moving Objects Using a Spatiotemporal Total Variation Regularization Algorithm, 18 (2018), Sensors 2018, 1704

[20] Celik N., Manivannan N., Strudwick A., and Balachandran W., Graphene-enabled electrodes for electrocardiogram monitoring,Nanomaterials, 6 (2016), No. 9.

[21] Gruetzmann A., Hansen S., and Müller J., Novel dry electrodes for ecg monitoring, Physiological Measurement, 28 (2007), No. 11, 1375.

[22] Searle A. and Kirkup L., A direct comparison of wet, dry and insulating bioelectric recording electrodes, Physiological Measurement, 21 (2000), No. 2, 271.

[23] Yapici M. K., Alkhidir T., Samad Y. A., and Liao K., Graphene-clad textile electrodes for electrocardiogram monitoring, Sensors and Actuators B: Chemical, 221 (2015), 1469 – 1474.

[24] Yapici M. K. and Alkhidir T. E., Intelligent medical garments with graphene-functionalized smart-cloth ecg sensors, Sensors, vol. 17 (2017), No. 4.

[25] Rymarczyk T., Characterization of the shape of unknown objects by inverse numerical methods, Przegląd Elektrotechniczny, 88 (2012), No 7b, 138-140

[26] Rymarczyk T., Szumowski K., Adamkiewicz P., Tchórzewski P., Sikora J., Moisture Wall Inspection Using Electrical Tomography Measurements, Przegląd Elektrotechniczny, 94 (2018), No 94, 97-100

[27] Majchrowicz M., Kapusta P., Jackowska-Strumiłło L., Sankowski D., Acceleration of image reconstruction process in the electrical capacitance tomography 3d in heterogeneous, multi-gpu system, Informatyka, Automatyka, Pomiary w Gospodarce i Ochronie Środowiska (IAPGOŚ) , 7 (2017), No. 1, 37-41;

[28] Rymarczyk T, Kłosowski G. Innovative methods of neural reconstruction for tomographic images in maintenance of tank industrial reactors. Eksploatacja i Niezawodnosc – Maintenance and Reliability, 21 (2019); No. 2, 261–267

[29] Rymarczyk T., Kłosowski G., Kozłowski E., Tchórzewski P., Comparison of Selected Machine Learning Algorithms for Industrial Electrical Tomography, Sensors, 19 (2019), No. 7, 1521

[30] Wajman R., Fiderek P., Fidos H., Sankowski D., Banasiak R., Metrological evaluation of a 3D electrical capacitance tomography measurement system for two-phase flow fraction determination, Measurement Science and Technology, 24 (2013), No. 6, 065302.

[31] Ye Z.., Banasiak R., Soleimani M., Planar array 3D electrical capacitance tomography, Insight: Non-Destructive Testing and Condition Monitoring, 55 (2013), No. 12, 675-680